THE HARD SOLAR X-RAY BURST OF 18 SEPTEMBER 1963

C. DE JAGER
University Observatory and Space Research Laboratory, Utrecht

(Received 29 May, 1967)

Abstract. A hard solar X-ray burst was observed by J-P. Legrand on 18 September 1963, 13:56 UT, at balloon altitude. It lasted a few minutes; a steep increase was followed by an exponential decay. During its declining phase a weak radio burst was observed on 3 and 10 cm, not on longer wavelengths.

Maximum radio intensity occurred two minutes after that of the X-ray burst. The X-ray and radio bursts ended almost simultaneously. Optically a small shortlived ($\lesssim$some minutes) flare point occurred simultaneously with the X-ray burst in a magnetically interesting part of the active region of September 1963. The X-burst photons seem to have had an energy of about 0.5 MeV. The burst was therefore of a fairly rare type, since very few other bursts with similar photon energies have been detected up to now.

It is suggested that a mass of gas, magnetically confined to a volume of about $5 \cdot 10^{25}$ cm^3 in the low corona, containing about $3 \cdot 10^{35}$ electrons was accelerated to energies of about 0.5 MeV. The gas gradually expanded, partly also to higher levels. The gyro-synchrotron radiation, emitted by the plasma became observable after about two minutes. At the lower radio frequencies the radiation was absorbed by overlying undisturbed coronal matter. Quantitative computations justify this model. A detailed summary of the events, and some numerical data are given in the concluding Section 8 and in Table V.

1. The X-Ray Phenomenon

A hard X-ray burst, most likely of solar origin, was detected with a Geiger-Müller telescope, flying at balloon altitudes near Kiruna (N. Sweden), on September 18, 1963. The balloon was instrumented and launched in the SPARMO cooperative program by a group of the 'Laboratoire de Physique Cosmique' at Meudon, under J-P. Legrand. A detailed description of the X-ray observations appeared elsewhere (De Jager and Legrand, 1965). The photons were recorded by a telescope consisting of three Geiger-Müller counters, in a setup now known as the SPARMO counter unit. This unit transmits the following data:

(a) pulses from the upper counter, type Victoreen 1B85 ('Al counter');
(b) pulses from the middle counter, type Victoreen 6306 ('Bi counter');
(c) coincidences between the upper and the lower counters.

The observations during the event are shown in Figure 1.

Since the number of coincidences (c) did not increase during the event, it is clear that the burst is due to photons, and not to an increased particle flux. Since furthermore the efficiency of the two counter types mentioned under (a) and (b) above differs (Figure 2), the average photon energies involved can be determined from the ratio between the excess counting rates of the two counters. It is clear from Figure 2 that as a rule one ratio of excess counting rates will yield two possible photon energies. For the present case we find the two values given in Table I. For this investigation we shall assume that the photon energy was either 65 or 500 keV.

Solar Physics 2 (1967) 327–346; © *D. Reidel Publishing Company, Dordrecht-Holland*

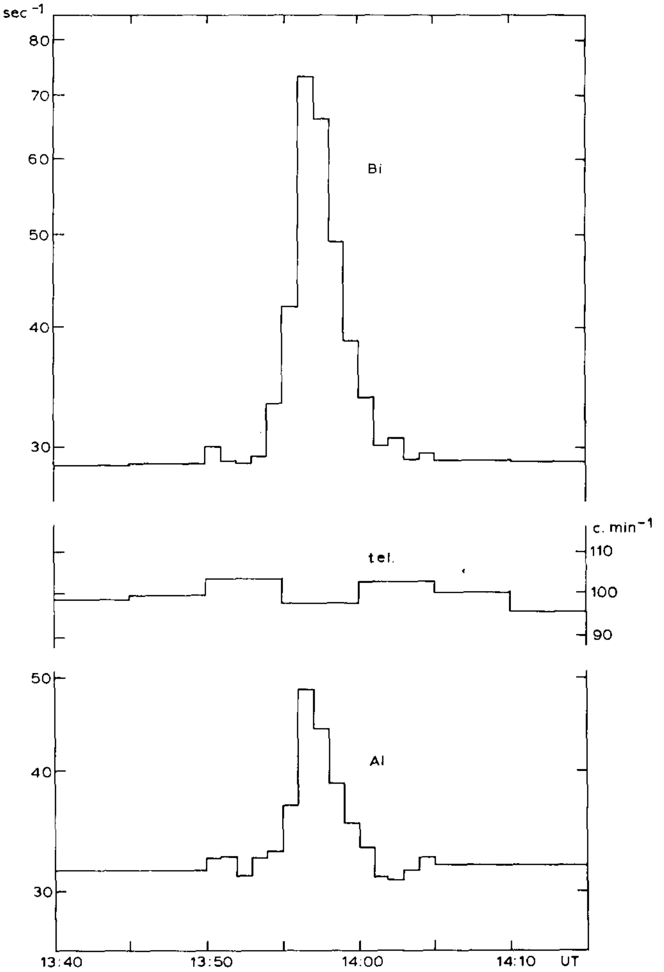

Fig. 1. Photon counts made during the hard X-ray event of 18 September 1963. Al: counts taken with the Victoreen counter 6306; Bi: counts taken with the Victoreen counter 1B85; telescope: counts taken with the particle telescope.

The following times characterize the event:

start at	13^h	54^m	$\pm 1^m$	UT
half maximum intensity at	13	56	± 0.3	
maximum at	13	56.5	± 0.3	
half maximum intensity at	13	58.5	± 0.3	
end at	14	01	± 1	

The observations reported here were the only X-ray observations of this event. No other observations came to our knowledge, and no other research groups were measuring hard solar X-rays at that time.

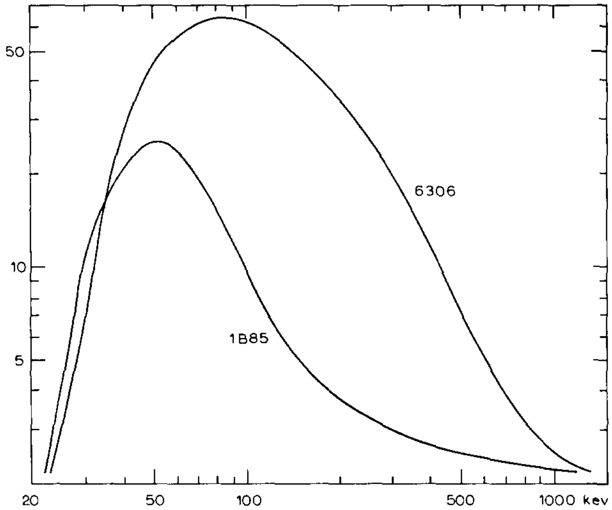

Fig. 2. Relative efficiencies of the Al and Bi counters.

TABLE I

Determination of the Average Photon Energy

time (UT)	excess counting rate (sec^{-1}) 6306	1B85	possible average energies (keV)	
13:54.5	4.5	1.3	70	450
:55.5	13.2	5.2	60	550
:56.5	44.6	17.0	60	550
:57.5	37.5	12.7	65	500
:58.5	20.4	7.1	65	500
:59.5	9.9	3.6	65	500

The number of photons incident on the earth during the event may next be estimated. Because of the ambiguity in the photon energy, all computations will be made for the two assumed energies (65 and 500 keV), until a decision can be made. The maximum effective area of the counters is 38 cm^2; however, since the orientation of the counters during the observation was unknown we have to use the average effective area, this being $\frac{1}{4}$ of the total superficial area, i.e. 24 cm^2. From Figure 1 we read the total number of pulses recorded by the Bi counter (Victoreen, type 6306), namely 8390 pulses. The number of photons passing through 1 cm^2 outside the earth's atmosphere at right angles to the direction of the sun, was found after applying corrections for atmospheric absorption and for counter efficiency. During the observations the balloon was floating at the 5.5 mbar level. The zenith distance of the sun was 71°.4. The atmospheric transmission t at 65 and 500 keV under these circumstances is 0.051 and 0.22, for 65 and 500 keV respectively. Furthermore, we have to take into account that 500 keV photons produce a large flux of scattered low energy photons. Taking the efficiency of the counter at these lower energies into account this multiplication factor at 5.5 m bar is estimated to be 25.*

At 65 and 500 MeV the top efficiency E of the Bi counter is estimated to be about 4%*, while the relative efficiencies η at 65 and 500 keV read from Figure 2, are 56% and 7% of the top efficiency. Hence, the incident number of photons is attenuated by the factor $E\eta t$, being $7 \cdot 10^{-4}$ or $3.8 \cdot 10^{-4}$, respectively.

Consequently the total number of photons emitted by the burst and incident on 1 cm^2 at the earth's distance, at right angles to the direction of the sun were $5 \cdot 10^5$ or $4 \cdot 10^4$, with a maximum rate of $2.6 \cdot 10^3$ or $2.0 \cdot 10^2$ photons cm^{-2} sec^{-1}.

Assuming isotropic solar emission, the total number of X-ray photons emitted during the event is $1.4 \cdot 10^{33}$ or $1 \cdot 10^{32}$, with a maximum rate of $7.4 \cdot 10^{30}$ or $5 \cdot 10^{28}$ sec^{-1}. The total X-ray energy emitted is $1.4 \cdot 10^{26}$ or $8 \cdot 10^{25}$ erg; the maximum rate is $7 \cdot 10^{24}$ or $4 \cdot 10^{24}$ erg sec^{-1}.

We also have to discuss whether the phenomenon was really of solar origin. Since the observations were made at high geomagnetic latitudes, during a period of high solar activity, the burst could also have been of auroral origin. Against the auroral hypothesis, and for the solar one we have the following arguments:

(1) The burst was a single one of unusually short duration; no auroral X-ray storm was going on at the instant of observation.

(2) The structure of the X-ray event, with its steep rise and exponential decay (Figure 3) was typical for solar phenomena, not for auroral bursts.

(3) The burst was associated with a solar radio burst (Section 3) and with solar optical emission (Section 4).

(4) The burst was associated with an ionospheric Sudden Frequency Deviation, observed in terrestrial equatorial regions (Section 2).

Though these associated phenomena were weak, they seem definitely to be associated with the X-ray event.

In Figure 3 the logarithm of the excess counts are plotted against the time interval Δt after the burst maximum. These counts show clearly that the burst intensity decreases *exponentially*; the intensity I can be represented by

$$I = \text{const.} \exp(-\Delta t(\text{sec})/86).$$

This observation *and* the steep rise of the burst to maximum intensity prove that the burst must have been caused by a *rapid excitation* followed by a kind of *relaxation process.*

2. Ionospheric Phenomena

About ten minutes after the burst a solar flare started, which reached its greatest intensity around 14:20 UT. Although at that latter moment some sudden ionospheric

---

* Thanks are due to Mr. H.F. van Beek, Space Research Laboratory, Utrecht, for providing me with these data.

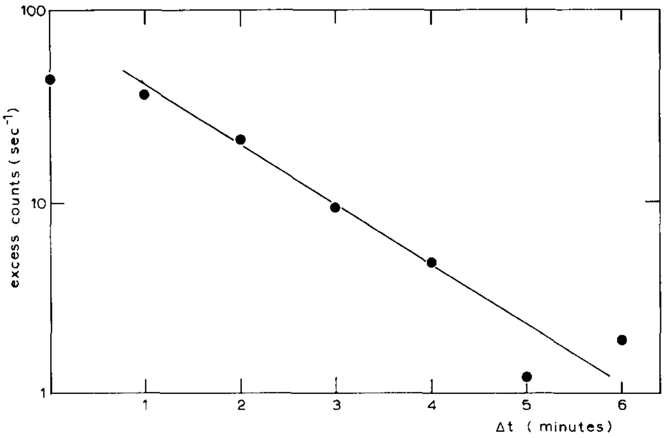

Fig. 3. Plot of the logarithm of the excess counting rate against time showing the exponential decay of the photon flux.

disturbances were noted, there was only one such event at the moment of the X-ray burst. There were:

no ionospheric absorptions (De Bilt, Lindau);
no Mögel-Dellinger effects (Nera);
no magnetic crochets (De Bilt);
no SFA's (De Bilt);
no SEA's (Uccle, Firenze).

These negative results show that either the energy of the X-ray photons was too large to be absorbed in atmospheric layers as high as the ionospheric D-region, or that the burst was too short-lived to significantly influence the D-region since the above-mentioned types of SID's depend on the time integral of the radiation enhancement.

The only type of SID that has been observed was a small 'Sudden Frequency Deviation' (SFD) with start, maximum and end approximately at 13:57, 13:58 and ≈14:00 UT (private communication by Dr. R.F. Donnelly, Space Disturbances Laboratory, ESSA, Boulder). The timing accuracy for start and maximum times is approximately ± 0.5 minute. The SFD reproduced in Figure 4 was observed on 10.1 MHz at the Monrovia-Accra communication, and on 20.2 MHz and 10.1 MHz transmitted from Monrovia and received at Natal, Brazil. It was not observed at Boulder, presumably because the SFD was small, the solar zenith angle in Boulder was large, and the ionosphere in Boulder was relatively disturbed. SFD's differ from most other SID's in that their sensitivity to the wavelength of the solar X radiation is not limited to the band between approximately 0.5–10 Å like for other SID's, but they seem to be sensitive to radiation enhancements in a broad band ranging from below 0.5 Å to the middle-ultraviolet, near 1000 Å. They react rather on the impulsivity of the solar burst (Donnelly, private comm.).

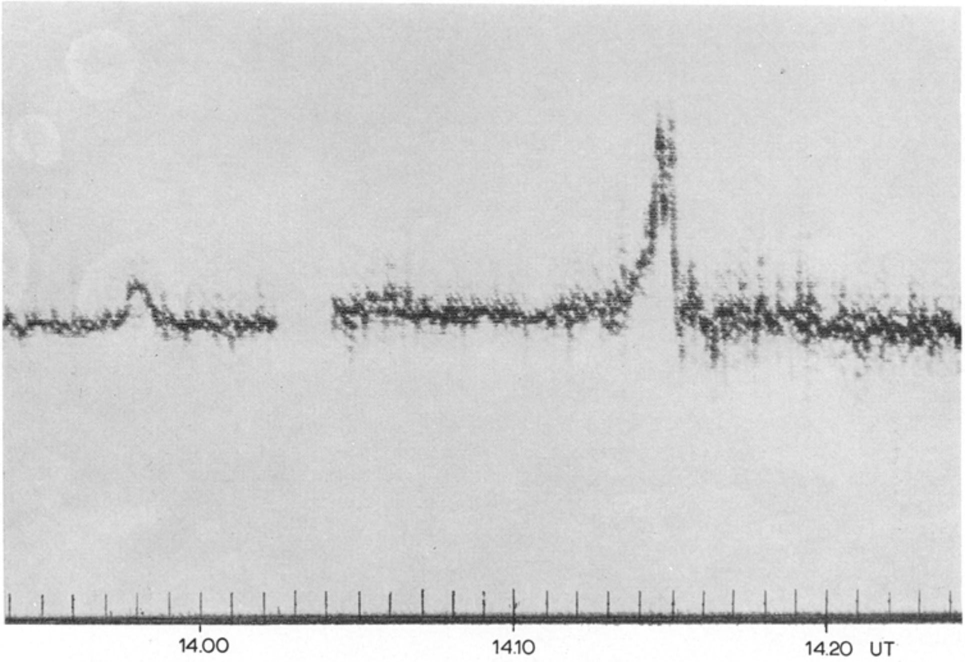

Fig. 4. Ionospheric Sudden Frequency Deviation observed between 13:57 and 14:00 UT at 10.1 MHz on the Monrovia-Accra communication. (By courtesy of R.F. Donnelly, Boulder.)

It may be significant that the characteristic times of the SFD agree better with those of the radio events (see Section 3, and Figures 5a,b, 6a,b, and 7) than with those of the X-ray burst. There appears to be a general time difference of about 2 minutes between the start and maximum times of the X-burst on one hand, and these times for the radio and ionospheric bursts. All features *end* at about the same time.

3. Radio Phenomena

There were *no* radio phenomena on meter or long dm waves associated with the X-ray burst. There was also no measurable enhancement of the radio noise on 15 and 20 cm (observations carried out at the 'Heinrich Herz Institut der Deutschen Akademie der Wissenschaften' at Berlin). The only wavelengths where response was obtained were those near 10 and 3 cm. No observations were made at wavelengths shorter than 3 cm.

Around 10 and 3 cm observations were secured at:

(1) the Radio and Electrical Engineering Division of the National Research Council of Canada (Covington, Ottawa) – 2800 MHz, Figure 5a;

(2) the Radio Astronomical Observatory NERA of the Netherlands P.T.T. (Fokker, Utrecht) – 2980 MHz, and 9100 MHz, Figures 5b and 6a;

(3) the 'Heinrich Herz Institut der Deutschen Akademie der Wissenschaften' at Berlin (Fürstenberg, Berlin) – 9400 MHz, Figure 6b.

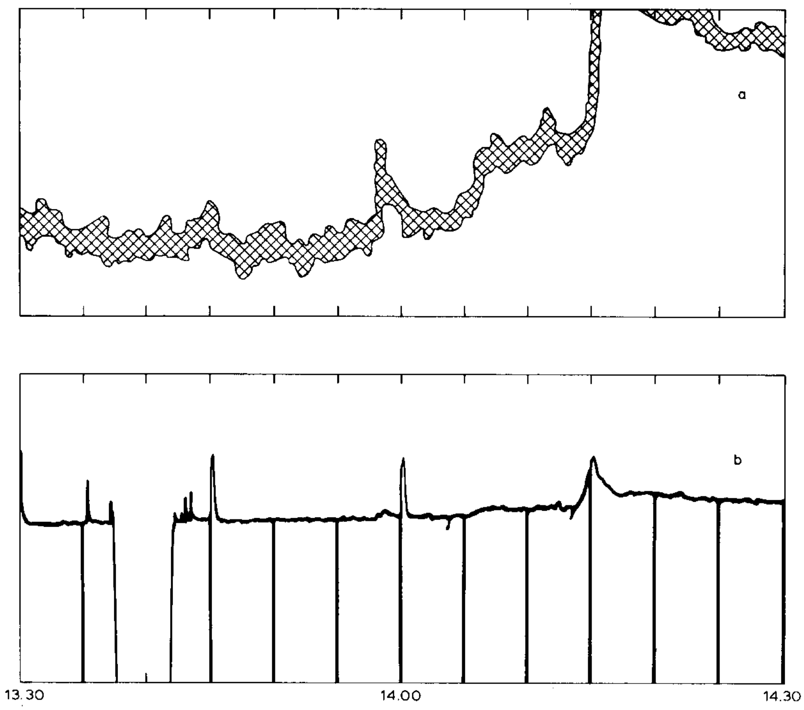

Fig. 5. (a) Radio-observations made at Ottawa at 2800 MHz. (By courtesy of A.E. Covington, National Research Council of Canada, Ottawa.) – (b) Radio-observations made at the Nera Observatory of the Netherlands P.T.T., at 2980 MHz. (By courtesy of A.D. Fokker, Utrecht.)

Some data pertinent to these observations are given in Table II.

The NERA recordings were obtained on faster moving recording charts than the others, so that they were useful for a fairly precise determination of the time of maximum intensity. However, since the NERA intensity scale was rather small the times of start and end and that of half intensity were difficult to measure. These latter data could be measured better on the recordings obtained in Berlin and Ottawa. Altogether Table II shows a fair agreement between the times of start, maximum and end, as read from the various radio recordings. In the 'Heinrich Herz Institut' observations (3.2 cm) there is some indication that the burst may be composed of a relatively long-lasting flat one starting $13^{\mathrm{h}}\ 56.9^{\mathrm{m}}$ and ending $14^{\mathrm{h}}\ 02.5^{\mathrm{m}}$, and a more spiky one starting $13^{\mathrm{h}}\ 57.9^{\mathrm{m}}$ and ending $14^{\mathrm{h}}\ 00.9^{\mathrm{m}}$. This is the meaning of the values in brackets in the fourth column of Table II.

Figure 7 gives a rough outline of the time histories of the X-ray and radio bursts. Apparently the radio burst started after the moment of maximum intensity of the X burst but all bursts ended about simultaneously. Like the X-ray burst the shape of the radio bursts seems asymmetric, as is clear from Table II.

The peak fluxes measured at the four wavelengths were determined as fractions of the quiet sun's noise level. For an internally consistent intercomparison of these

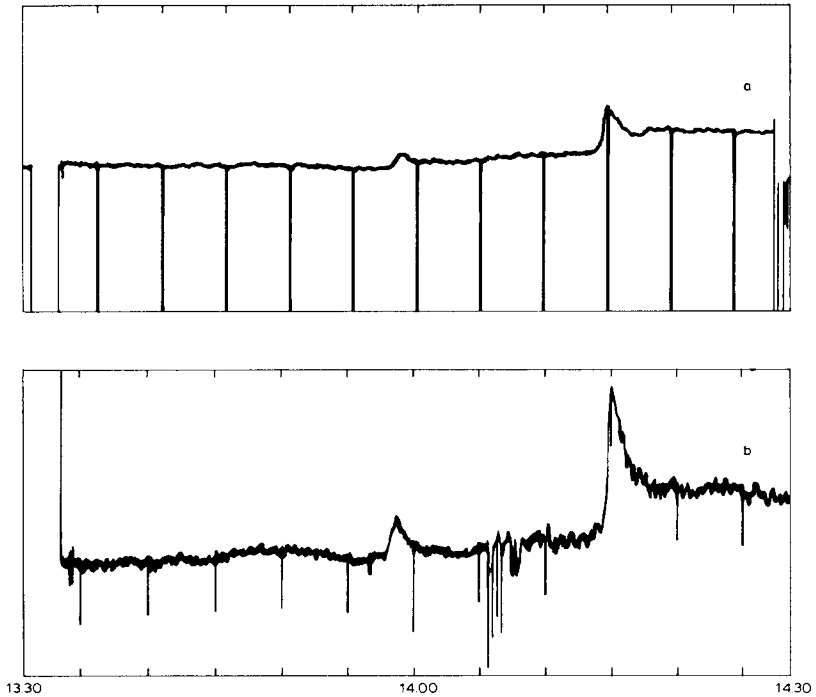

Fig. 6. (a) Radio-observations made at the Nera Observatory of the Netherlands P.T.T., at 9100 MHz. (By courtesy of A.D. Fokker, Utrecht.) – (b) Radio-observations made at the 'Heinrich Herz Institut der Deutschen Akademie der Wissenschaften', at 9400 MHz. (By courtesy of F. Fürstenberg, Berlin-Adlershof.)

TABLE II

Characteristic Times of the Radio Events (expressed in minutes after 13^h UT)

frequency (MHz) observatory	2800 Ottawa	2980 Nera	9100 Nera	9400 Berlin
start	57	57.8	57.8	57.9 (56.9)
half intensity	58.4	—	58.3	58.1
maximum	58.4	58.8	58.8	58.8
half intensity	60.0	59.4	59.4	59.6
end	61.5	—	60.8	60.9 (62.5)

four peak fluxes we have transformed them into absolute intensities by means of an assumed quiet sun spectrum, taken from ALLEN (1963). Since the sun was not completely quiet during the burst, but showed at least one important active region, we assumed a 'quiet sun spectrum' intermediate between the spectra for maximum and minimum activity.

For the 'quiet' sun's flux we took:

at 2900 MHz: $S = 90$ Jansky;
at 9250 MHz: $S = 320$ Jansky.

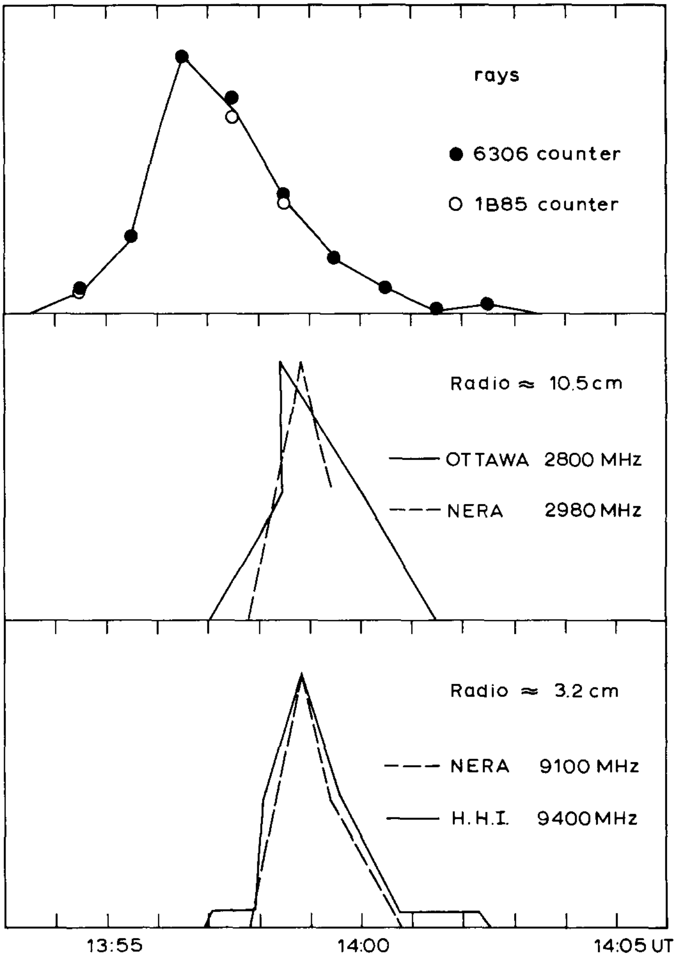

Fig. 7. Relation between the time histories of the X-ray and radio bursts.

A possible error in this assumption would affect both results in the same way and would therefore hardly change our conclusions in the later part of this paper. The resulting peak fluxes are given in Table III.

TABLE III

Radio Peak Fluxes observed at 3 and 10 cm.

frequency	relative flux (%)	absolute peak fluxes (Watt m^{-2} Hz^{-1})
2800 (Ottawa)	5.5	$5 \cdot 10^{-22}$
2980 (Nera)	4.5	$4 \cdot 10^{-22}$
9100 (H.Herz Inst.)	6	$19 \cdot 10^{-22}$
9400 (Nera)	6	$19 \cdot 10^{-22}$

4. Optical and Magnetic Phenomena during the Event

A more detailed discussion of the optical and magnetic observations relevant to the event will be given in our later publication. Yet it is important for the present investigation to mention some characteristics of the active region from where the burst most likely originated. There was one very active region on the sun, the famous region of September 1963; described by ZIRIN and WERNER (1967). All major activity of September 18, 1963 was confined to this region, so that the X-ray burst must certainly also have found its origin there.

The active region was of the hour glass shape, which is typical for flares emitting high-energy phenomena. See Figure 8. Magnetographic observations by TESKE *et al.* (1964) and by SEVERNY (unpublished, kindly communicated) show the bright filament in the neck of the hour glass, near the point Z in Figure 9, fully to coincide with a region where the electric field vector is parallel to the solar surface (the 'neutral line'). One cannot help seeing this bright filament as a large horizontal magnetic flux tube in the spot group. Furthermore the gradient of the horizontal field strength was very large in the region around this filament.

Professor Kiepenheuer kindly communicated the following list of flares which occurred around the time of the X-ray event:

heliographic location	times (UT)	importance	observatory
14N 24E	12:33–13:40	1+	Stockholm
11N 25E	13:23–**13:35**	1−	Sacramento Peak
13N 25E	**14:07–14:50**	1	Sacramento Peak
10N 25E	14:10–15:00	2+	McMath-Hulbert
12N 25E	14:11–14:45	2	Freiburg

He added: "Die ausführlichsten Beobachtungen wurden vom Sacramento Peak gemacht und zwar ununterbrochen von 13:23 bis 15:47, offenbar 4 Bilder/Minute. Nach Sacramento Peak begann die Eruption **14:07** und endete **14:50**. Daraus würde folgen, dass der X-ray burst *vor* dem Eruptionsanfang in Hα stattfand."

In their paper, Zirin and Werner do mention the flare of 14:07, but they also find some earlier activity, concurrent in time with the X-ray phenomenon. This is shown in Figure 10. There was a small bright point (called a flare in Zirin and Werner's paper) in the bright filament in the neck of the hour glass at 13:57 UT (the point Z in Figure 9); at the same time a flare spray occurred to the left of the facula. The bright point did not last longer than a few minutes and, hence, coincided fairly well in time with the X-ray maximum. It looks attractive to associate the active center at Z with the source of the X-ray event and with the primordial acceleration process;

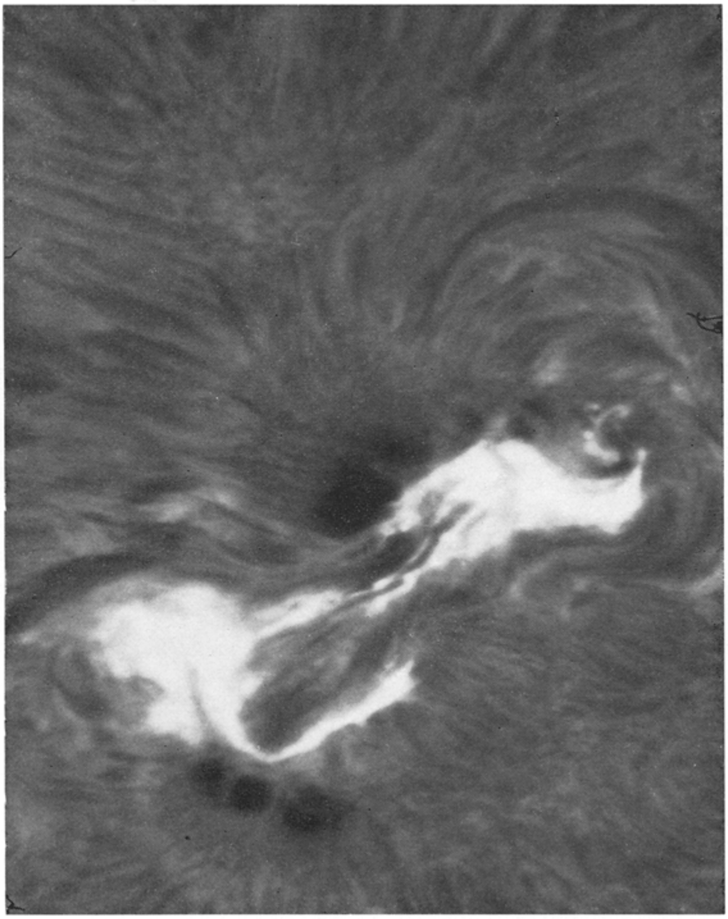

Fig. 8. The active region of 18 September 1963. The picture was taken through a 0.55 Å filter centered at H$\alpha \pm 0.0$ Å with an exposure time of $0^s.1$ at 14:36:10 UT by dr. J. M. Beckers at the Sacramento Peak Observatory, Air Force Cambridge Research Laboratories. One mm = $0''.7$.

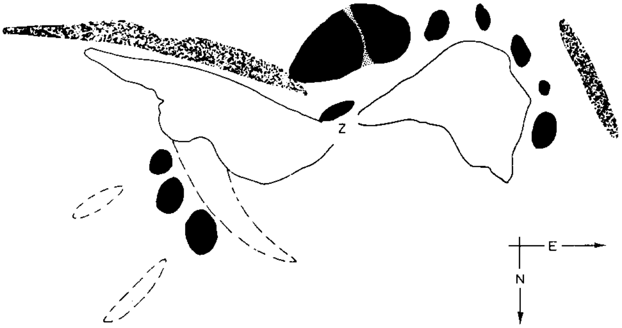

Fig. 9. Schematic drawing of the sunspots and faculae in the active region of September 1963. The drawing has been taken from Zirin and Werner (1967), Figure 4b, p. 72.

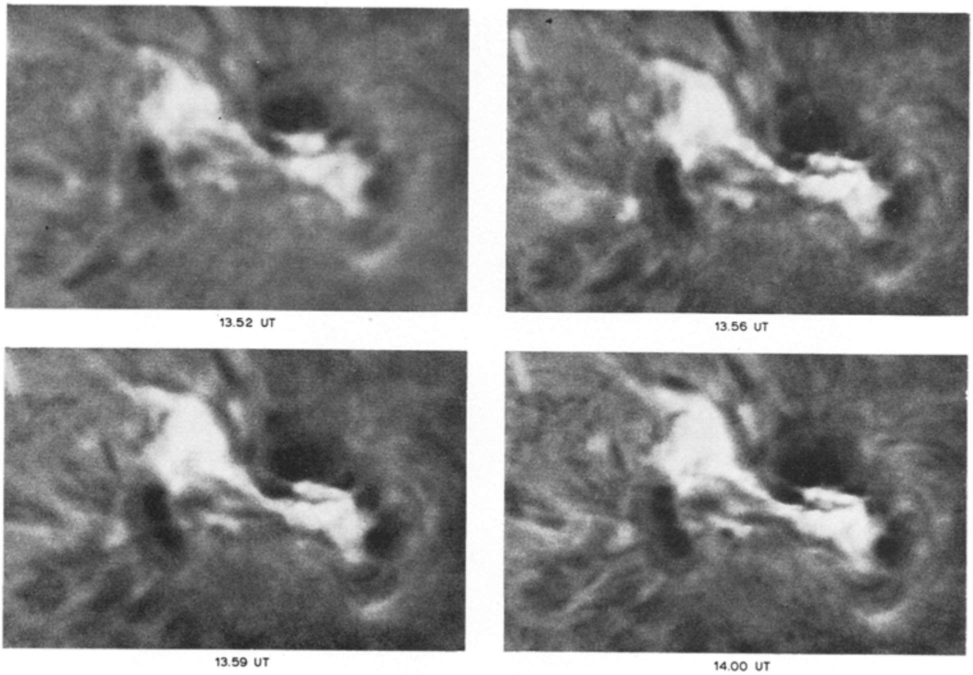

13.52 UT

13.56 UT

13.59 UT

14.00 UT

Fig. 10. Four Hα filtergrams showing the development of the active region around the time of the X-ray and radio bursts. Note the bright points in the neck of the facular hourglass at 13:56 UT and the small surge-like feature in the left hand part of the figure at 13:56 and still faintly visible at 13:59 UT. (By courtesy of H. Zirin, Pasadena.)

furthermore it may not appear impossible to associate the longer-lasting spray with the second phase of the X-ray event and/or with the radio event. See further in ZIRIN and WERNER (1967), Figure 4, Table III, Figure 14 and the relevant text.

In the next two sections we shall use the radio- and X-ray observations to derive some general relations between the various parameters which describe the state of the gas. At the same time this will enable us further to elaborate the model described here.

5. Discussion of the X-Ray Observations

With the X-ray observations we are still up against the ambiguity of the two possible photon energies (65 or 500 keV). Hence, all computations will be made for the two energies until a decision can be made.

A first point to be discussed is the mechanism of X radiation. The observed X-ray flux must be due to bremsstrahlung. Other mechanisms, such as the inverse Compton effect or electron-positron annihilation (at 500 keV) look less probable. Also the synchrotron mechanism can easily be ruled out, since it would demand far too strong magnetic fields to be efficient in the hard X-ray region.

The total X-ray energy, emitted during the whole burst was $1.4 \cdot 10^{26}$ (for 65 keV) or $8 \cdot 10^{25}$ erg (for 500 keV).

The total energy loss by bremsstrahlung can be estimated with an expression given by SCHATZMAN (1965):

$$E_{\mathrm{rad}} \approx 3.10^{-10}\, y^2 \text{ ergs/electron},$$

where y is the ratio between the kinetic energy and the rest-energy of the electron. Hence, assuming the photon-energy to be approximately equal to the initial kinetic energy of the electrons one obtains the number of electrons $\int Ne\, \mathrm{d}V$, given in Table V.

Furthermore it is possible to derive the *number density of the electrons* of the ambient gas from the observed decay of the X-ray burst. Since the shape of the tail of the burst can be represented by $\exp(-\Delta t/86 \text{ sec})$ the stopping time in the gas must be about 86 seconds. An expression for this stopping time t_s has been derived by SCHATZMAN (1965), who found:

$$t_s = \frac{\sqrt{2}}{3c}\, y^{3/2} A_e^{-1}, \tag{1}$$

where c is the velocity of light, y has been defined already, and

$$A_e = 1.14 \cdot 10^{-24} [2N_e(13.68 + \tfrac{1}{2} \log T/N_e + \log y) + N_0(4.84 + \log y)].$$

Here N_e and N_0 are the electron- and heavy particle-density in the ambient gas. This expression can be simplified if we assume the number of heavy particles N_0 to be equal to N_e (complete ionisation). We assume further that $T = 3 \cdot 10^8$ °K for a gas with 65 keV electrons, and $2.5 \cdot 10^9$ °K for 500 keV electrons. This assumption is not critical at all since T enters only in the logarithm term; an error of a factor 10^3 in T makes only an error of 10% in the resulting N_e-value. Then, the expression for A_e becomes:

$$A_e = 1.14 \;\; 10^{-24} N_e \left(32.20 + 3 \log y + \log \frac{T}{N_e}\right) \tag{2}$$

From Equations (1) and (2), taking for t_s the observed value 86 seconds, one obtains the following values for N_e^*, the electron density in the ambient gas:

photon energy:	65	500 keV
$A_e =$	$8.6 \cdot 10^{-15}$	$1.83 \cdot 10^{-13}$
$\log N_e^* =$	8.4	9.7

This result leads immediately to an important conclusion, *viz.* that the relevant electrons are confined by a magnetic field. Electrons of 65 or 500 keV have mean velocities of 0.47 c and 0.87 c. In 86 seconds they would cover distances of $12 \cdot 10^6$ or $22 \cdot 10^6$ km. Along a straight path they would have arrived in a part of the corona where the electron and proton densities are of the order of $2.5 \cdot 10^3$ or 10^3 cm^{-3} respectively, which is much smaller than the above-found values for the ambient gas density.

It is now also possible to derive a minimum value for the volume V occupied by the accelerated electrons. If we assume that the ambient electron density N_e^* is equal to the electron density N_e of the accelerated component of the gas, hence, if we assume that a part of the corona is just *as a whole* accelerated to high energies, then one obtains the minimum volume of the gas.

For a photon energy of	65	or	500 keV,
one has	$V \geqq 1.4 \cdot 10^{29}$	or	$5 \cdot 10^{25}$ cm^3;
for a sphere the radius would be	$R \geqq 32000$	or	2400 km.

6. Discussion of the Radio Observations

In this section we investigate the possibility that the observed radio bursts are due to thermal radiation of a gas with kinetic temperature T, electron density N_e and thickness Z in the line of sight. For such a gas the emitted radiation flux F at a frequency f is:

$$F = B(1 - e^{-\kappa Z}), \tag{1}$$

where B is the source function:

$$B = 2\pi c^{-2} k T f^2, \tag{2}$$

and κ is the absorption coefficient per cm (see Kundu, 1965, p. 40):

$$\kappa = N_i N_e \frac{16\pi}{3} \frac{e^6}{c} \frac{1}{(2\pi m k)^{3/2}} \frac{1}{f^2 T_e^{3/2}} \ln \left\{ \frac{8k^3 T^3}{\pi^2 e^4 f^2 m} - 5\gamma \right\}. \tag{3}$$

With $N_i N_e = 10/11 N_e^2$ (assuming 10% He), the expression (3) reduces to

$$\kappa \approx 0.1 N_e^2 f^{-2} T_e^{-3/2}, \tag{3a}$$

for the cm region and normal coronal conditions, and for $T = 10^7$ °K and $f = 9250$ MHz it becomes

$$\kappa \approx 0.4 N_e^2 f^{-2} T_e^{-3/2}. \tag{3b}$$

It is clear from Equations (1) to (3) that the observed radio emission cannot be the thermal emission of an optically thick plasma, because the observations show:

$$\frac{d \log F}{d \log f} = 1.2,$$

whereas for an optically thick plasma the value of this gradient is equal to 2, and for an optically thin plasma it would be equal to 0. So it seems that three possibilities remain:

(a) the gas may be in a transitory state between optically thin and optically thick;

(b) the radio emission of an optically thin or nearly thin plasma is partly absorbed by the overlying corona, leading to the change of the spectral shape;

(c) the radiation is not thermal.

In this section we shall examine cases (a) and (b) and we will show that neither case (a) nor case (b) lead to an acceptable solution while case (c) does (Section 7).

Case (a); intermediate optical thickness without coronal absorption:

Starting form the observed gradient d log$F$/ d log$f=1.2$, and assuming the known ratio between the absorption coefficients ($\sim f^{-2}$), one readily finds for the total optical depths τ ($=\kappa Z$) at the two average frequencies:

$$\begin{aligned} 2900\ \text{MHz}&: \tau = 5.4;\\ 9250\ \text{MHz}&: \tau = 0.53. \end{aligned} \tag{4}$$

The thermal radio spectrum, computed with Equation (1) and the above values for the optical depths is drawn as a dashed line in Figure 11.

The result (4) has been derived from the peak intensities of the radio burst and is consequently valid for the instant (13:58.5 UT) at which that intensity was emitted.

Next we examine the meaning of the derived optical thicknesses. We write $\tau=\kappa Z$, where Z is the geometrical thickness of the plasma cloud. We now write $f=2.9\cdot 10^9$ Hz, $\tau=5.4$, $N_e=2.5\cdot 10^7$ or $5\cdot 10^9$ (see Section 6), and obtain

$$\begin{array}{lrl} \text{for} & N_e = 2.5\cdot 10^8 & 5\cdot 10^9 \\ & T_e^{-3/2} Z \quad 1.9\cdot 10^3 & 4.7 \\ \text{for } T_e = 2\cdot 10^6\,{}^\circ\text{K}: & Z = 5\cdot 10^7\ \text{km} & 130000\ \text{km} \\ \quad 10^7\,{}^\circ\text{K} & 6\cdot 10^8\ \text{km} & 1400000\ \text{km} \end{array}$$

These resulting values for Z are extremely large and can not be reconciled with the observation that *no* radio burst was recorded at wavelengths of 15 cm and longer, which should have been the case for any Z larger than about 30000 km. Also, this geometrical configuration of the cloud (very long, extremely thin tube pointing towards the earth) would be highly improbable. Therefore we conclude that the assumption (a) is not correct.

Case (b); thin plasma with coronal absorption:

We now assume the plasma to be optically thin. From the discussion in case (a) it is obvious that in order to have $Z \lesssim 30000$ km, the optical depth at 2900 MHz should in any case be smaller than 10^{-3} to 10^{-4} for the case $N_e=2.5\cdot 10^8$ and smaller than 10^{-1} for $N_e=5\cdot 10^9$. In these cases the radio spectrum of the plasma itself is flat: d log$F$/d log$f=0$. The influence of coronal absorption is given by an exponential factor $e^{-\tau}$, where τ is the optical thickness of the overlying corona. Since $\tau \sim f^{-2}$ a short computation shows that the observed radio spectrum is represented by coronal optical thicknesses:

$$\begin{aligned} \tau &= 1.66 \text{ at } 2900\ \text{MHz}, \quad \text{and}\\ \tau &= 0.16 \text{ at } 9250\ \text{MHz}. \end{aligned}$$

However, it can easily be shown, that these results are not consistent either:

For an optically thin cloud with volume V the radiation flux would be, according to Equations (1), (2) and (3):

$$F=\kappa B \approx 0.8\pi C^{-2} N_e^2 k T^{-\frac{1}{2}}\cdot V.$$

Solving this equation with the given value V and the given flux values yields $T \approx 50\,°\mathrm{K}$! This means that the observed radio flux is apparently much too intense to be explained by thermal emission, and that we have to look for a more powerful emission mechanism, like gyro-synchrotron emission.

7. The hypothesis of gyro-synchrotron emission

Since the electrons are certainly confined by a magnetic field (see section 5) they *must* emit radiation of the gyro-synchrotron type. For electron energies of 65 and 500 keV the v/c values are 0.45 and 0.87 respectively. At these energies the radiation should be emitted at discrete frequencies characterized by the gyrofrequency $f_H = 2.8\mathrm{H}$ MHz, and its harmonics. Here H is the magnetic field in gauss. However due to Doppler effect obliteration the resulting gyro-synchrotron spectrum is surely continuous as a detailed computation showed. The upper part of Table IV gives the computed intensity ratio of the gyro-synchrotron emission F_{2900}/F_{9250}. The computations are made both for the extra-ordinary and for the ordinary emission. The lower part of Table IV gives the optical depth of the overlying coronal region, necessary to explain the observed intensity ratio at the two wavelengths. It is clear that a coronal absorption, characterized by an optical depth of 1.0 to 1.7 is sufficient to explain the observed spectrum. For the time being we assume an optical depth of the overlying corona of 1.7, which is the value for the ordinary radiation.

TABLE IV

Investigation of the gyro-synchrotron case

Upper part: computed intensity ratio of the gyro-synchrotron emission F^{2900}/F^{9250}. E = extra-ordinary emission; O ordinary emission.

Lower part: optical depth of the overlying coronal gas, necessary to explain the observed intensity ratio at the two frequencies

H	750	1000	1500	Gauss
E+O	2.2	2.5	2.2	
O	4.0	4.8	4.0	
E	1.8	2.0	1.8	
E+O	1.08	1.24	1.08	
O	1.73	1.85	1.73	
E	0.85	0.97	0.85	

The spectrum computed with these optical thicknesses is shown as a solid line in Figure 11.

In order to examine the meaning of these values we write $\tau = \kappa H$, where H is the coronal scale height, and where κ is taken from Equation (3a), which equation is representative for normal coronal conditions. In that case the N_e values to be used in

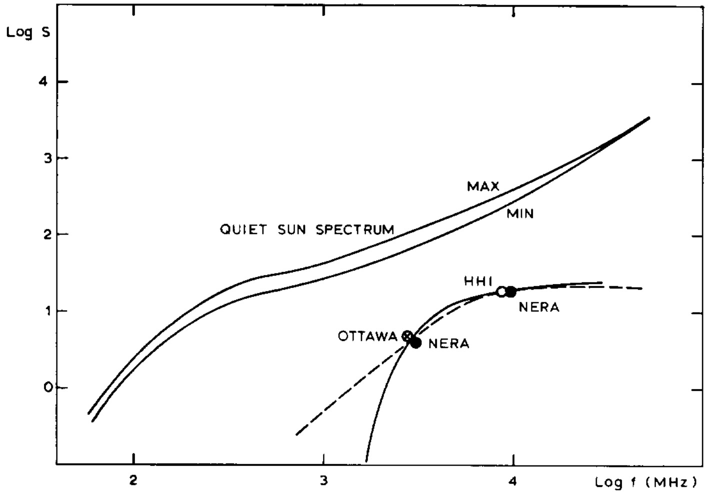

Fig. 11. Radiospectra of the sun and the active region. Abscissa: $\log f$ in MHz; ordinate: $\log S$ in Jansky. Solid lines: the quiet sun's general radio spectrum. Dashed: suggested thermal burst spectrum, case (a); Solid: gyro-synchrotron spectrum attenuated by the overlying corona.

Equation (3a) should be those valid at the basis of the overlying corona, just above the plasma cloud.

Hence we have to solve N_e from the equation: $\tau = 0.1\ N_e^2 f^{-2}\ T_e^{-3/2}\ H$.

With $T = 10^6$ °K, $H = 50000$ km we find $N_e = 5.3 \cdot 10^9$ cm^{-3};
with $T = 1.5 \cdot 10^6$ °K, $H = 75000$ km we find $N_e = 4.3 \cdot 10^9$ cm^{-3};
with $T = 10^4$ °K, $H = 500$ km we find $N_e = 1.7 \cdot 10^9$ cm^{-3}.

It is very gratifying to see that *these* electron densities are virtually equal to those found for the densities *in* the plasma cloud for electron energies of 500 keV (Section 6). So there is in this picture no discontinuity between the densities in the plasma cloud and those at the basis of the overlying corona, which is just the most natural situation.

8. Conclusions

The results of the previous analysis are summarized in Table V, which gives the derived values of the various quantities for the two assumed photon energies.

We are now able to come to a decision about the photon energies. To that end we visualize the geometrical configuration. The position of the cloud with respect to the sun may be found through the ambient electron density N_e^*. With the given relation between the coronal electron density and the height in the corona (De Jager, 1959, p. 271), and assuming that in an active region the electron density is approximately 10 times the quiet coronal density it is found that $N_e = 2.5 \cdot 10^8$ occurs at heights of 200000 km above the sun, while an electron density of $5 \cdot 10^9$ occurs at the transition between chromosphere and corona, about 5000 to 10000 km above the photosphere.

We also found (Table V) the volumes of the two kinds of clouds.

TABLE V

Result of the Analysis

assumed photon energy		65	500	keV
emission per electron		$4.2 \cdot 10^{-12}$	$3 \cdot 10^{-18}$	erg
observed total emission		$1.4 \cdot 10^{26}$	$8 \cdot 10^{25}$	erg
total number of electrons	$\int N_e \, dV$	$3.4 \cdot 10^{37}$	$3 \cdot 10^{35}$	
ambient electron density	N_e^*	$2.5 \cdot 10^{8}$	$5 \cdot 10^{9}$	cm^{-3}
minimum volume	V_{min}	$1.4 \cdot 10^{29}$	$5 \cdot 10^{25}$	cm^3
minimum cloud radius	R_{min}	32000	2400	km

Clearly the 500 keV cloud is small and comparable in size to the part of the active region where the acceleration process is likely to take place. The 65 keV cloud has to be located at a fairly great distance from the sun and it looks improbable that at such a distance from the active region the acceleration of a large amount of electrons to an energy of 65 keV could take place in about one minute.

Hence, the geometrical configuration argues for the 500 keV cloud. There are other arguments. There were some optical phenomena in the active region at the very moment of the X-ray burst. This could be understood if the source of the burst could have been located at a small distance to the active region as should be the case with the 500 keV cloud. It would be highly improbable to have optical phenomena in the active region if the region of particle excitation would be located as far from the active region as the 65 keV cloud.

Another fairly strong argument was given in Section 7, where it was shown that the density at the basis of the coronal regions just above the excited plasma cloud had to be $5 \cdot 10^9$ cm^{-3}, just equal to the density *in* the cloud for the 500 keV case.

Taking these arguments together it seems certain that the excited part of the corona has contained electrons with energies of 500 keV rather than of 65 keV. Clearly these values should only be taken as approximately true; in deriving the energy values we have assumed the photons to be strictly monochromatic, which is not necessarily correct. However, also in the case of a broader photon spectrum, the derived values for the photon energies should be taken as approximately indicating the average value.

Because of these high photon energies the burst is of a fairly rare type. Up to now, only four bursts have been detected with photon energies of that order (DE JAGER, 1967).

Altogether a *summarizing picture* of the succession of the events may be as follows. A hard X-ray burst of solar origin was observed between 13:56 and 14:01 UT with a maximum on 13:56.5 UT. A steep rise was followed by an exponential decay. The most probable photon energy was approximately 0.5 MeV. At the time of the X-ray burst there was a sudden flash-like brightening of a few points in the facular field. The brightening lasted not much longer than one or a few minutes, comparable to the duration of the first part of the X-ray burst. The points were situated on a bright line connecting two bright patches of the facular field. This line happened to be identical with the magnetic field vector at this place; furthermore the field gradient at right angles was very large.

It is suggested that at that time some electromagnetic mechanism accelerated the electrons . The acceleration period, as judged from the rise time of the burst and from the duration of the point-like brightening, may have been of the order of one minute. The electrons lost their energy by bremsstrahlung and thus produced the X-ray burst. The total emitted X-ray energy is $8 \cdot 10^{25}$ erg; the collision time in the plasma was 86 seconds, which explains the exponential decay time of the burst. The electron density ($\approx$ proton density) of the gas was slightly less than 10^{10} cm^{-3}. The total number of electrons involved was $3 \cdot 10^{35}$; the gas contained a volume which, if supposed spherical, had a radius of 2400 km. The gas gradually expanded to higher levels, and eventually it produced a gyro-synchrotron radio burst, which could be observed about 2 minutes after the X-ray burst and ended simultaneously with it. At that time the gas could also have emitted a quasi-thermal soft X-ray burst in the wavelength region between approximately 1 and 10Å, but this could not be observed since there were no soft X-ray monitoring satellites active during this event. However, the observed ionospheric SFD (Figure 4) may be an indication that such radiation was indeed emitted.

Acknowledgements

I am greatly indebted to many colleagues who put their observational data so generously at my disposal. This investigation is completely based on their observations. *The X-ray observations* were obtained from: dr. J-P. Legrand, Meudon.

Hα filtergrams were received from: dr. J.M. Beckers, Sacramento Peak Observatory; dr. R. Coutrez, Uccle-Brussels; dr. H. Dodson-Prince, McMath Hulbert Obs.; dr. J.W. Evans, Sacramento Peak Observatory; dr. J.W. Firor, Boulder; dr. K.O. Kiepenheuer, Freiburg im Br. ; and dr. H. Zirin, Pasadena.

Radio observations were obtained from: dr. A.E. Covington, Ottawa; dr. R. Coutrez, Uccle-Brussels; dr. H. Daene, Potsdam; dr. A.D. Fokker, Utrecht; dr. Fürstenberg, Berlin-Adlershof; dr. L. Krivsky, Ondřejov; and dr. G. Righini, Arcetri-Firenze.

Ionospheric data were obtained from: dr. J. Veldkamp (De Bilt); dr. W. Dieminger (Lindau); dr. A.D. Fokker (Nera); dr. R. Coutrez (Uccle); dr. G. Righini (Firenze); and dr. R.F. Donnelly (Boulder).

Magnetographic recordings were sent by: dr. A.B. Severny, Crimean Observatory.

Finally it is a pleasure to thank ir H.F. van Beek, dr. H.G. van Bueren, dr. A. D. Fokker, dr. T. Takakura and mr. G. Moreton for their helpful suggestions and fruitful discussions on the subject. I am very greatly indebted to mr. R. Snijders (Space Research Laboratory, Utrecht) for help in some computations, and for many stimulating comments.

References

ALLEN, C.W.: 1963: *Astrophysical Quantities*, 2nd ed. Attlone Press, London.

De Jager, C.: 1959, in *Handbuch der Physik*, vol. **52**. Springer Verlag, Berlin.

De Jager, C.: 1967, in *Electromagnetic Radiation in Space* (ed. by J.G. Emming). Reidel, Dordrecht. See also *Solar Physics* **2**, 347.

De Jager, C. and Legrand, J.P.: 1965, *SPARMO bulletin* **3**, 1–3.

Kundu, M.R.: 1965, *Solar Radio Astronomy*. Interscience Publishers, New York.

Schatzman, E.: 1965, in *The Solar Spectrum* (ed. by C. de Jager). Reidel, Dordrecht, p. 313.

Teske, R.G., Dodson, H., and Hedeman, E.R.: 1964, *Astrophys. J.* **139**, 1336.

Zirin, H. and Werner, S.: 1967, *Solar Physics* **1**, 66.